Supporting Online Material

MD99-2227 Age Model

For TI, our age model for MD99-2227 is based on 10 planktonic radiocarbon dates from MD99-2227 (reported in Fagel et al., 2004), supported by 13 planktonic radiocarbon dates transferred from the adjacent core HU90-013-013 (Fig. 1) (reported in Stoner et al., 1995; Evans et al., 2007) to MD99-2227 using their magnetic susceptibility records (Stoner et al., 1995) and the techniques of Stoner et al. (2007) (see Fig. DR1 & Table DR1). All ages are reservoir corrected and calibrated with CALIB 5.0.2. We also used the timing of Heinrich Event 2 (H2) at 23.5 to 24.5 cal kyr BP in our age model as indicated by the abrupt increase in percent $CaCO_3$ (Fig. 2d).

For TII, our age model is based on maximizing the correlation of MD99-2227 relative paleo-intensity records (Evans et al., 2007) to Site 983 in the North Atlantic (Channell et al., 1997) placed on the Site 1089 chronology from the South Atlantic (Stoner et al., 2003). This age model is originally derived from orbital tuning of the 1089 benthic $\delta^{18}O$ (Hodell et al., 2001; Stoner et al., 2003) and is therefore as robust as any other paleoclimate record for this time interval. However, comparisons between these records and other paleoclimate and sea level records should be considered as tentative until dating techniques are improved beyond the limits of radiocarbon. The agreement between the timing of H11 in MD99-2227 of ~130 to 128 kyr BP (Fig. 2c) and the H11 radiometric date of ~129 kyr BP (Shackleton et al., 2002) suggests that the MD99-2227 TII age model could be as accurate as ±1000 years.

Sediment Source Determination

There are two possible terrestrial sediment sources to the Eirik Drift: the southern Greenland Precambrian Shield and sediment transported in the Western Boundary Under Current (WBUC), including Tertiary basalts of Iceland and east Greenland (Fig. 1) (Fagel et al., 2002; 2004). Basalts have a higher [Fe] relative to [Ti] and felsic rocks are enriched in [Ti] relative to [Fe] (Steenfelt, 2001). XRF measured weight percent Ti and Fe concentrations in stream sediment from streams draining basaltic terrane in west Greenland (basalts similar to those of east Greenland and Iceland) have a Ti/Fe ratio of ~0.1 (Steenfelt, 2001). Stream sediment from the felsic terrane of southern Greenland have a Ti/Fe ratio of ~0.3, also measured by XRF (Steenfelt, 2001). The agreement between Ti and Fe, and the larger signal in Ti relative to Fe thus suggest that the majority of terrestrial sediment reaching MD99-2227 is mainly derived from felsic sources, the closest of which is the southern Greenland Precambrian Shield (Steenfelt, 2001). Mafic rocks also contain a component of Ca in plagioclase feldspar. However, the excellent agreement between the XRF measured [Ca] and % $CaCO_3$ (Fig. DR3) indicates that Ca is predominately of biogenic and/or detrital carbonate origin. Principal component analysis of XRF measured [Ti], [Fe], [Ca], and [Sr] (see below) determined that the fourth empirical orthogonal function with opposite loadings of Fe and Ti is likely WBUC-transported material from east Greenland and Iceland basalts. However, it shows reduced deglacial variability (Fig. DR3) and only explains < 0.1 % of the overall variability. In addition, the WBUC did not reach its full velocity until after ~7 k.y. BP following the end of Northern Hemisphere deglaciation (Hillaire-Marcel et al., 2001; Fagel et al., 2002; 2004), and was reduced relative to its modern intensity during TII and subsequent interglacial (Hillaire-Marcel et al., 2001). Thus the geochemical changes in our records likely do not reflect changes in the amount of WBUC-delivered sediment, rather changes in the input of proximally-derived sediment from southern Greenland.

Interpreting Ti and Fe Concentration Data

As indicated in the manuscript, the interpretation of increased [Ti] and [Fe] (after correcting for Ca dilution) as reflecting southern Greenland Ice Sheet (sGIS) retreat is supported by modern observations (Hallet et al., 1996) and previous interpretations of a similar record (Lamy et al., 2004). Lamy et al. (2004) suggested that increased [Fe] in a core proximal to the Patagonian Ice Sheet (PIS) could reflect enhanced sediment input during deglaciation due to the mechanisms discussed in the manuscript: the exposure of glacial sediment to erosion by ablation and runoff that is transported to the ocean, with greater retreat exposing more sediment to these processes. Lamy et al. also suggested, and used in their final interpretation, that increased [Fe] represented PIS advances because peaks in [Fe] aligned with PIS margin maxima dated by Denton et al. (1999). However, recalibration of these maxima ^{14}C ages places them on average ~500 to 1000 years earlier than the calibrated ages of Lamy et al. (Fairbanks et al., 2005). The new timings of PIS margin maxima are actually at Fe concentration minima with Fe input increasing during deglaciation. Thus, the new calibrated dates would support the first interpretation of the [Fe] record of Lamy et al. (2004), similar to our interpretation of the MD99-2227 [Ti] and [Fe] data as records of summer sGIS ablation and runoff from southern Greenland. We note that this interpretation is similar to inferences from XRF measured Ti and Fe concentration records of precipitation and stream discharge to the

Cariaco Basin during the Holocene and glacial period (Peterson et al., 2000; Haug et al., 2001).

Principal Component Analysis

We used our XRF measured [Ti], [Fe], [Sr] and [Ca] as variables in a principal component analysis. The four empirical orthogonal functions (EOF) scores are shown in Figure DR4 along with the loading coefficients for Ti, Fe, Sr and Ca. EOF1 is related to Sr and Ca variability and, given its similarity to % $CaCO_3$, is most likely the biogenic and detrital carbonate signal. Ti and Fe correspond the strongest with EOF2 and likely reflect terriginous, felsic sediment input from southern Greenland. EOF3 has opposite loadings in Sr and Ca, and may reflect changes in carbonate chemistry. EOF4 has opposite loadings in Fe and Ti. Because an increase in Fe with a relative decrease in Ti is predicted by the input of Western Boundary Undercurrent (WBUC) transported sediment (Fagel et al., 2002; 2004), we attribute this EOF as a recorder of volcanic sediment input (WBUC transported sediment).

References

Channell, J.E.T., Hodell, D.A., and Lehman, B., 1997, Relative geomagnetic paleointensity and δ18O at ODP Site 983 (Garder Drift, North Atlantic) since 350 ka: Earth and Planetary Science Letters, v. 153, 103-118.

Denton, G.H., Lowell, T.V., Heusser, C.J., Schlüchter, C., Andersen, B.G., Heusser, L.E., Moreno, P.I., and Marchant, D.R., 1999, Geomorphology, stratigraphy, and radiocarbon chronology of Llanquihue Drift in the area of the Southern Lake

District, Seno Reloncaví, and Isla Grande de Chiloé, Chile: Geografiska Annaler, v. 81, p. 167-229.

Evans, H.F., Channell, J.E.T., Stoner, J.S., Hillaire-Marcel, C., Wright, J.D., Neitzke, L.C., and Mountain, G.S., 2007, Paleointensity-assisted chronostratigraphy of detrital layers on the Eirik Drift (North Atlantic) since marine isotope stage 11: Geochemistry, Geophysics, Geosystems, v. 8, doi: 10.029/2007GC001720.

Fagel, N., Hillaire-Marcel, C., Humblet, M., Brasseur, R., Weis, D., and Stevenson, R., 2004, Nd and Pb isotope signatures of the clay-size fraction of Labrador Sea sediments during the Holocene: Implications for the inception of the modern deep circulation pattern: Paleoceanography, v. 19, doi: 10.1029/2003PA000993.

Fagel, N., Inocent, C., Gariepy, C., and Hillaire-Marcel, C., 2002, Sources of Labrador Sea sediments since the last glacial maximum inferred from Nd-Pb isotopes: Geochmica et Cosmochimica Acta, v. 66, p. 2569-2581.

Fairbanks, R.G., and 9 coauthors, 2005, Radiocarbon calibration curve spanning 0 to 50,000 years BP based on paired $^{230}Th/^{234}U/^{238}U$ and ^{14}C dates on pristine corals: Quaternary Science Reviews, v. 24, p. 1781-1796.

Haug, G.H., Hughen, K.A., Sigman, D.M., Peterson, L.C., and Röhl, U., 2001, Southwards migration of the Intertropical Convergence Zone through the Holocene: Science, v. 293, p. 1304-1308.

Hillaire-Marcel, C., deVernal, A., Bilodeau, G., and Weaver, A.J., 2001, Absence of deep-water formation in the Labrador Sea during the last interglacial period: Nature, v. 410, p. 1073-1077.

Hodell, D.A., Charles, C.D., and Sierro, F.J., 2001, Late Pleistocene evolution of the ocean's carbonate system: Earth and Planetary Science Letters, v. 192, p. 109-124.

Lamy, F., Kaiser, J., Ninnemann, U., Hebbeln, D., Arz, H.W., and Stoner, J., 2004, Antarctic timing of surface water changes off Chile and Patagonian Ice Sheet response: Science, v. 304, p. 1959-1962.

Peterson, L.C., Haug, G.H., Hughen, K.A., and Röhl, U., 2000, Rapid changes in the hydrologic cycle of the Tropical Atlantic during the last glacial: Science, v. 290, p. 1947-1951.

Shackleton, N.J., Chapman, M., Sánchez-Goñi, M.F., Pailler, D., and Lancelot, Y., 2002, The classic marine isotope Substage 5e: Quaternary Research, v. 58, p. 14-16.

Steenfelt, A., 2001, Geochemical atlas of Greenland – West and South Greenland: Geological Survey of Denmark and Greenland, Report 2001/46, 40 pp.

Stoner, J.S., Channell, J.E.T., and Hillaire-Marcel, C., 1995, Magnetic properties of deep-sea sediments off southwest Greenland: Evidence for major differences between the last two deglaciations: Geology, v. 23, p. 241-244.

Stoner, J.S, Channell, J.E.T., Hodell, D.A., and Charles, C.D., 2003, A ~580 kyr paleomagnetic record from the sub-Antarctic South Atlantic (Ocean Drilling Program Site 1089): Journal of Geophysical Research, v. 108, doi: 10.1029-2001JB001390.

Stoner, J.S., Jennings, A., Kristjansdottir, G.B., Dunhill, G., Andrews, J.T., and Hardardottir, J., 2007, A paleomagnetic approach toward refining Holocene radiocarbon-based chronologies: Paleoceanographic records from the north

Iceland (MD99-2269) and east Greenland (MD99-2322) margins: Paleoceanography, v. 22, doi: 10.1029/2006PA001285.

Table DR1. Calibrated radiocarbon dates used in age model construction for MD99-2227 (CALIB 5.0.2). Top set are from MD99-2227. Bottom set are dates transferred to 2227 using k_{ARM}/k records from the two cores (see Figure S1). Noted are the depths in 2227 to which 013 dates were transferred.

Figure DR1. MD99-2227 and HU90-013-013 k_{ARM}/k records on depth scales (Stoner et al., 1995; Evans et al., in review). Black dots denote radiocarbon dates for each core with calibrated mid point age (Stoner et al., 1995; Fagel et al., 2004). Dashed lines denote the transfer of 013 ages to 2227 depth.

Figure DR2. Linear regression of [Ca] versus [Ti] (red symbols, dashed line) and [Fe] (yellow symbols, solid line). The inverse relationship is mainly the glacial-interglacial change in biogenic productivity. We determined the inverse linear relationship between Ca – Ti and Ca – Fe, converted [Ca] into its effect on [Ti] and [Fe] using these linear relationships, and then divided Ti and Fe by the converted Ca record. Thus, when Ca is high, we divide by a smaller number and Ca is low, we divide by a larger number. This calculates the relative abundance of Ti and Fe in the sediment and removes the dilution effects of Ca.

Figure DR3. XRF [Ca] record (red) and % CaCO3 (black with symbols) from MD99-2227 on depth scale. Note the excellent agreement between the two records indicating that Ca is predominately sourced from biogenic and detrital carbonate, and not from volcanic sources.

Figure DR4. Principal component analysis of Ti, Fe, Sr and Ca XRF measured concentration after log-normalization. (**a**) The first EOF (EOF1) represents biogenic and detrital carbonate input due to strong loadings in Ca and Sr and opposite sign loadings in

Ti and Fe. (**b**) The second EOF (EOF2) is representative of southern Greenland runoff due to the strong loading in Ti and slightly lesser in Fe. (**c**) The third EOF (EOF3) has opposite loadings in Sr and Ca, and may represent changes in carbonate source. (**d**) The fourth EOF (EOF4) likely represents the WBUC with positive loading in Fe and negative loading in Ti. Note that it does not vary significantly during TI and TII.

TABLE DR1. RADIOCARBON DATES

MD99-2227 Radiocarbon Dates

Depth (cm)	^{14}C Age	Calibrated	Error*
0	1230	740	60
50	2625	2220	60
100	3690	3510	130
150	4565	4680	100
200	5640	5970	60
250	6335	6740	70
350	8300	8690	100
450	9490	10320	180
550	12510	13970	190
600	15750	18260	580

HU-90-013-013 Radiocarbon Dates

Depth (cm)	^{14}C Age	Calibrated	Error*	Depth 2227
190	6810	7670	180	267
210	7580	8370	190	283
240	7790	8600	200	335
340	8830	9890	300	435
360	9230	10420	190	459
370	10040	11550	300	467
390	10430	12350	350	495
400	10720	12730	160	507
420	11990	13860	210	535
430	12450	14540	420	570
440	12560	14660	430	575
450	14150	16890	470	590
480	16990	20130	220	625

*2 sigma error

Table DR1

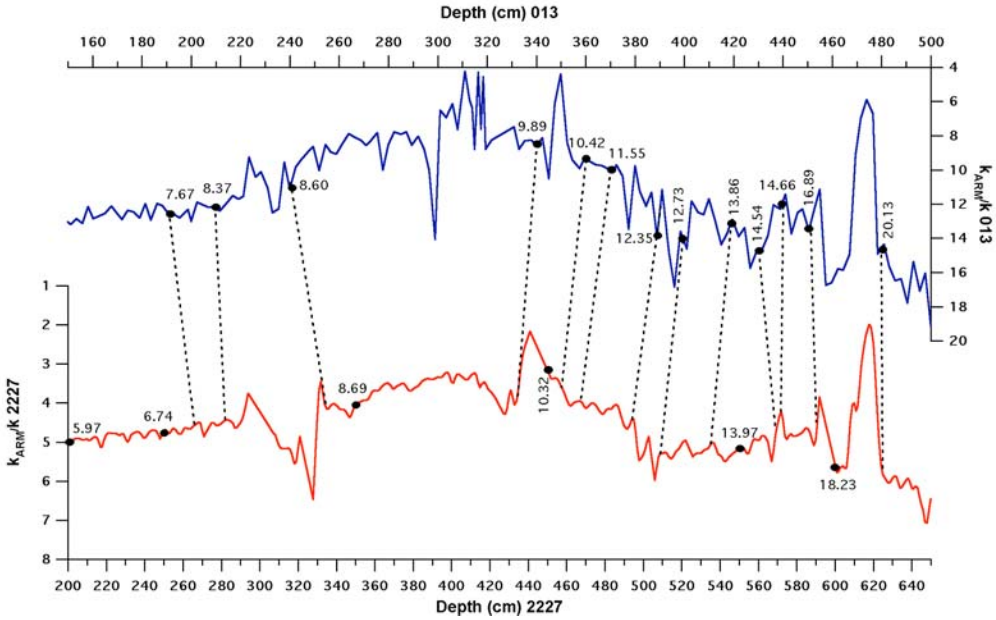

Depth (cm) 013
160 180 200 220 240 260 280 300 320 340 360 380 400 420 440 460 480 500
4 6 8 10 12 14 16 18 20
k_ARM/k 013
7.67
8.37
8.60
9.89
10.42
11.55
12.35
12.73
13.86
14.54
14.66
16.89
20.13
5.97
6.74
8.69
10.32
13.97
18.23
1 2 3 4 5 6 7 8
k_ARM/k 2227
200 220 240 260 280 300 320 340 360 380 400 420 440 460 480 500 520 540 560 580 600 620 640
Depth (cm) 2227

Figure DR1

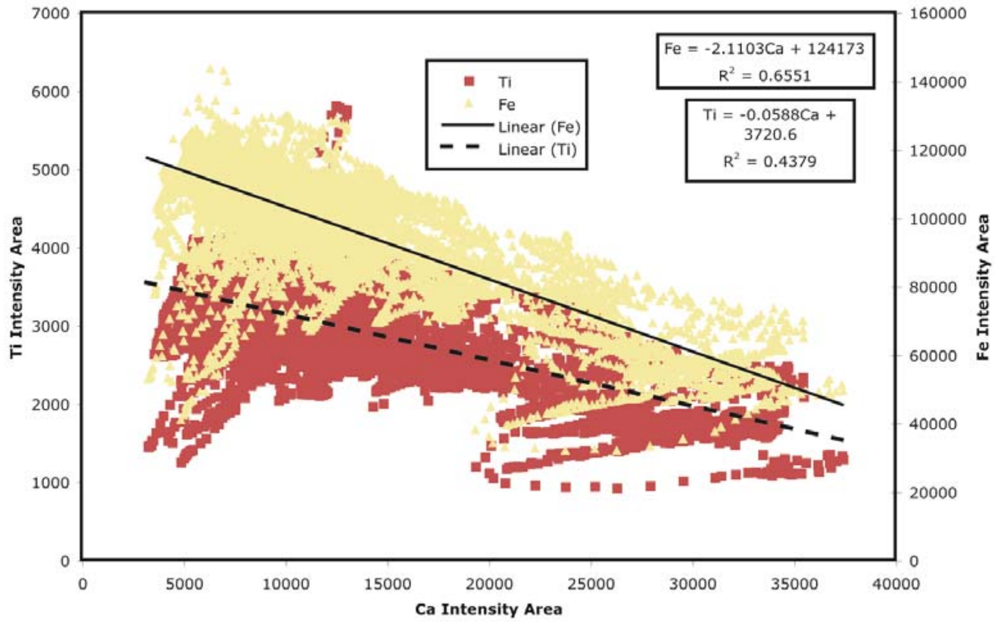
Fe = -2.1103Ca + 124173
R^2 = 0.6551
Ti = -0.0588Ca + 3720.6
R^2 = 0.4379
Ti
Fe
Linear (Fe)
Linear (Ti)
Ti Intensity Area
Fe Intensity Area
Ca Intensity Area
0
1000
2000
3000
4000
5000
6000
7000
20000
40000
60000
80000
100000
120000
140000
160000
5000
10000
15000
20000
25000
30000
35000
40000

Figure DR2

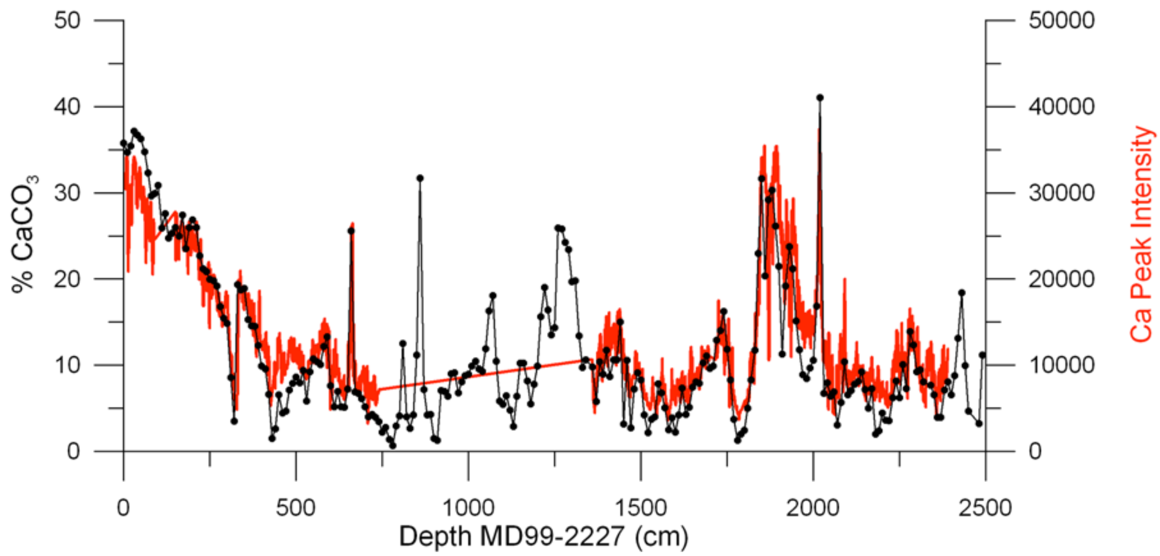
50
40
30
20
10
0
% $CaCO_3$
50000
40000
30000
20000
10000
0
Ca Peak Intensity
0
500
1000
1500
2000
2500
Depth MD99-2227 (cm)

Figure DR3

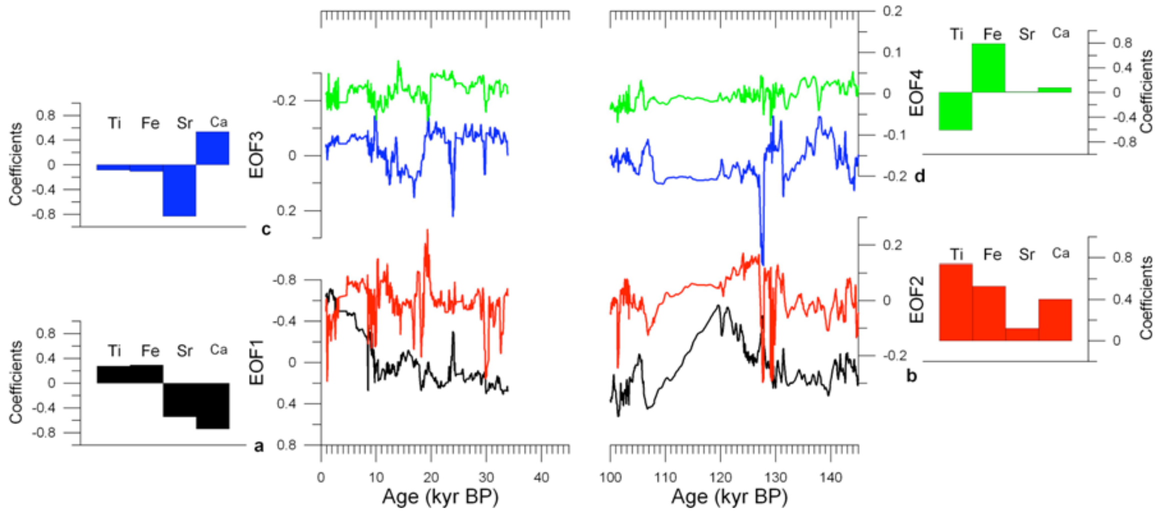
Coefficients
0.8
0.4
0
-0.4
-0.8
Ti Fe Sr Ca
c
a
EOF3
EOF1
EOF4
EOF2
d
b
Age (kyr BP)
Age (kyr BP)

Figure DR4